

ON THE EFFICIENCY OF RANDOM WALK APPROACH TO NOISE REDUCTION IN COLOR IMAGES

B. Smolka * M. Szczepanski *

Silesian University of Technology
Department of Automatic Control
Akademicka 16 Str, 44-101 Gliwice, Poland
bsmolka@ia.polsl.gliwice.pl

K.N. Plataniotis A. N. Venetsanopoulos

Edward S. Rogers Sr. Department of
Electrical and Computer Engineering
University of Toronto
10 King's College Road, Toronto, Canada
kostas@dsp.toronto.edu

ABSTRACT

In this paper we propose a new algorithm of noise reduction in color images. The new technique of multichannel image enhancement is capable of reducing impulse and Gaussian noise and it outperforms the basic methods based on vector median used for the noise reduction in color images. In the paper a new smoothing operator, based on a random walk model and on a fuzzy similarity measure between pixels connected by a digital geodesic path is introduced. The efficiency of the proposed method was tested on the standard color images using the widely used objective image quality measures.

1. STANDARD NOISE REDUCTION FILTERS

Most popular nonlinear, multichannel filters are based on the ordering of vectors in a predefined moving window [1-6]. The output of these filters is defined as the lowest ranked vector according to a specific vector ordering technique.

Let $\mathbf{F}(x)$ represent a multichannel image and let W be a window of finite size n (filter length). The noisy image vectors inside the filtering window W are denoted as \mathbf{F}_j , $j = 0, 1, \dots, n-1$. If the distance between two vectors $\mathbf{F}_i, \mathbf{F}_j$ is denoted as $\rho(\mathbf{F}_i, \mathbf{F}_j)$ then the scalar quantity $R_i = \sum_{j=0}^{n-1} \rho(\mathbf{F}_i, \mathbf{F}_j)$, is the distance associated with the noisy vector \mathbf{F}_i . The ordering of the R_i 's: $R_{(1)} \leq \dots \leq R_{(n-1)}$, implies the same ordering to the corresponding vectors \mathbf{F}_i : $\mathbf{F}_{(1)} \leq \dots \leq \mathbf{F}_{(n-1)}$. Nonlinear ranked type multichannel estimators define the vector $\mathbf{F}_{(0)}$ as the filter output. However, the concept of input ordering, initially applied to scalar quantities is not easily extended to multichannel data, since there is no universal way to define ordering in vector spaces.

To overcome this problem, distance functions are often utilized to order vectors. As an example, the *Vector Median Filter* (VMF) uses the L_1 or L_2 norm to order vectors according to their relative magnitude differences. The orien-

tation difference between two vectors can also be used to remove vectors with atypical directions (*Vector Directional Filter* - VDF, *Basic Vector Directional Filters* - BVDF).

The reduction of image noise without major degradation of the image structure is one of the most important problems of the low-level image processing. A whole variety of algorithms has been developed, but none of them can be seen as a final solution of the noise problem and therefore a new filtering technique, which copes better with impulsive and Gaussian noise has been proposed.

2. NEW ALGORITHM OF NOISE REDUCTION

Let us assume, that R^2 is the Euclidean space, W is a planar subset of R^2 and x, y are points of the set W .

A path from x to y is a continuous mapping $\mathcal{P}: [a, b] \rightarrow X$, such that $\mathcal{P}(a) = x$ and $\mathcal{P}(b) = y$. Point x is the starting point and y is the end point of the path \mathcal{P} [8-10].

An increasing polygonal line P on the path \mathcal{P} is any polygonal line $P = \{g(\lambda_i)\}_{i=0}^n$, $a = \lambda_0 < \dots < \lambda_n = b$. The length of the polygonal line P is the total sum of its constitutive line segments $L(P) = \sum_{i=1}^n \rho(\mathcal{P}(\lambda_{i-1}), \mathcal{P}(\lambda_i))$, where $\rho(x, y)$ is the distance between the points x and y , when a specific metric is adopted.

If \mathcal{P} is a path from x to y then it is called rectifiable, if and only if $L(P)$, where P is an increasing polygonal line is bounded. Its upper bound is called the length of the path \mathcal{P} . The geodesic distance $\rho^W(x, y)$ between points x and y is the lower bound of the length of all paths leading from x to y totally included in W . If such paths do not exist, then the value of the geodesic distance is set to ∞ . The geodesic distance verifies $\rho^W(x, y) \geq \rho(x, y)$ and in the case when W is a convex set then $\rho^W(x, y) = \rho(x, y)$.

The notion of the geodesic distance can be extended to a lattice, which is a set of discrete points, in our case image pixels.

Let a digital lattice $\mathcal{H} = (\mathbf{F}, \mathcal{N})$ be defined by \mathbf{F} , which is the set of all points of the plane (pixels) of a color im-

* This work was partially supported by KBN grant 8 T11E 013 19

age) and the neighbourhood relation \mathcal{N} between the lattice points.

A digital path $P = \{p_i\}_{i=0}^n$ on the lattice \mathcal{H} is a sequence of neighbouring points $(p_{i-1}, p_i) \in \mathcal{N}$. The length $L(P)$ of digital path P $\{p_i\}_{i=0}^n$ is simply $\sum_{i=1}^n \rho^{\mathcal{H}}(p_{i-1}, p_i)$. If $P(x, y)$ denotes the digital path connecting the points x and y in F then the lattice distance between those points is defined as $\rho^{\mathcal{H}}(x, y) = \min_{P(x, y)} L[P(x, y)]$.

Constraining the paths to be totally included in a pre-defined set $W \in \mathbf{F}$ yields the digital geodesic distance ρ^W . In this paper we will assign to the distance of neighbouring points the value 1 and will be working with the 8-neighbourhood system.

Let the pixels (i, j) and (k, l) be called connected, denoted as $(i, j) \leftrightarrow (k, l)$, if there exists a geodesic path $P^W\{(i, j), (k, l)\}$ contained in the set W starting from (i, j) and ending at (k, l) (Fig. 1).

If two pixels (x_0, y_0) and (x_n, y_n) are connected by a geodesic path $P^W\{(x_0, y_0), (x_1, y_1), \dots, (x_n, y_n)\}$ of length n then let χ

$$\chi^{W,n}\{(x_0, y_0), (x_n, y_n)\} = \sum_{k=0}^{n-1} \|\mathbf{F}(x_{k+1}, y_{k+1}) - \mathbf{F}(x_k, y_k)\| \quad (1)$$

be a measure of dissimilarity between pixels (x_0, y_0) and (x_n, y_n) , along a specific geodesic path P^W joining (x_0, y_0) and (x_n, y_n) . If a path joining two distinct points x, y , such that $\mathbf{F}(x) = \mathbf{F}(y)$ consists of lattice points of the same values, then $\chi^{W,n}(x, y) = 0$ otherwise $\chi^{W,n}(x, y) > 0$.

Let us now define the similarity function between two pixels connected along all geodesic digital paths leading from (i, j) and (k, l) (Fig. 1) [7]

$$\mu^{W,n}\{(i, j), (k, l)\} = \frac{1}{\omega} \sum_{l=1}^{\omega} \exp \left[-\beta \cdot \chi_l^{W,n}\{(i, j), (k, l)\} \right] \quad (2)$$

where ω is the number of all geodesic paths connecting (i, j) and (k, l) . β is a parameter and $\chi_l^{W,n}\{(i, j), (k, l)\}$ is a dissimilarity value along a specific path from a set of all ω possible paths leading from (i, j) to (k, l) . In this way $\mu^{W,n}\{(i, j), (k, l)\}$ is an average value, taken over all routes joining the starting point (i, j) and the end point (k, l) .

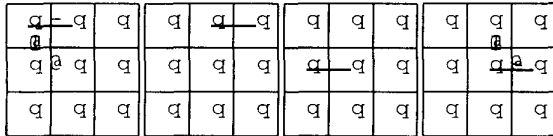


Fig. 1. There are four geodesic paths of length 2 connecting two neighbouring points contained in the 3×3 window W when the 8-neighbourhood system is applied.

For $n = 1$ and W a square mask of the size 3×3 , we have $\mu^{W,1}\{(i, j), (k, l)\} = \exp \{-\beta \|\mathbf{F}(i, j) - \mathbf{F}(k, l)\|\}$ and when $\mathbf{F}(i, j) = \mathbf{F}(k, l)$ then $\chi^{W,n}\{(i, j), (k, l)\} = 0$, $\mu\{(i, j), (k, l)\} = 1$, and for $\|\mathbf{F}(i, j) - \mathbf{F}(k, l)\| \rightarrow \infty$ then $\mu \rightarrow 0$.

The normalized similarity function takes the form

$$\psi^{W,n}\{(i, j), (k, l)\} = \frac{\mu^{W,n}\{(i, j), (k, l)\}}{\sum_{(l, m) \leftrightarrow (i, j)} \mu^{W,n}\{(i, j), (l, m)\}} \quad (3)$$

The normalized similarity function has the property

$$\sum_{(k, l) \leftrightarrow (i, j)} \psi^{W,n}\{(i, j), (k, l)\} = 1 \quad (4)$$

Now we are in a position to define a smoothing transformation \mathcal{J}

$$\mathcal{J}(i, j) = \sum_{(k, l) \leftrightarrow (i, j)} \psi^{W,n}\{(i, j), (k, l)\} \cdot \mathbf{F}(k, l) \quad (5)$$

where (k, l) are points which are connected with (i, j) by geodesic digital paths of length n included in W .

3. RESULTS

The effectiveness of the new smoothing operator defined by (5) was tested using the *LENA* and *PEPPERS* standard images contaminated by Gaussian noise of $\sigma = 30$. We also used the *LENA* image contaminated by 4% impulsiv noise (salt & pepper added on each channel) mixed with Gaussian noise ($\sigma = 30$).

The performance of the presented method was evaluated by means of the objective image quality measures RMSE, PSNR, NMSE and NCD [3]. Tables 2 and 3 show the obtained results for $n = 3$ and β increasing linearly from 10 to 30. After 3 iterations the filtered image was being sharpened and was visually more pleasing, however the quality measures were decreasing. Therefore only the results of 3 iterations are shown in the Tab. 2 and 3. Additionally Fig. 2 shows the comparison of the new filtering technique with the standard vector median.

For the calculation of the similarity function we used the L_1 metric and an exponential function, however we have obtained good results using other convex functions and different vector metrics.

4. CONCLUSIONS

In this paper, a new filter for noise reduction in color images has been presented. Experimental results indicate that the new filtering technique outperforms standard procedures used to reduce mixed impulsive and Gaussian noise in color images. The efficiency of the new filtering technique is shown in Tables 2 and 3.

Notation	Filter
AMF	Arithmetic Mean Filter
VMF	Vector Median Filter
BVDF	Basic Vector Directional Filter
GVDF	Generalized Vector Directional Filter
DDF	Directional-Distance Filter
HDF	Hybrid Directional Filter
AHDF	Adaptive Hybrid Directional Filter
FVDF	Fuzzy Vector Directional Filter
ANNF	Adaptive Nearest Neighbor Filter
ANP-EF	Adaptive Non Parametric (Exponential) Filter
ANP-GF	Adaptive Non Parametric (Gaussian) Filter
ANP-DF	Adaptive Non Parametric (Directional) Filter
VBAMMF	Vector Bayesian Adaptive Median/Mean Filter

Table 1. Filters taken for comparison with the proposed filter [1-5].

5. REFERENCES

- [1] A.N. Venetsanopoulos, K.N. Plataniotis, Multichannel image processing, Proceedings of the IEEE Workshop on Nonlinear Signal/Image Processing, 2-6, (1995)
- [2] I. Pitas, A. N. Venetsanopoulos, 'Nonlinear Digital Filters : Principles and Applications', Kluwer Academic Publishers, Boston, MA, (1990)
- [3] K.N. Plataniotis, A.N. Venetsanopoulos, 'Color Image Processing and Applications', Springer Verlag, (June 2000)
- [4] I. Pitas, P. Tsakalides, Multivariate ordering in color image processing, IEEE Trans. on Circuits and Systems for Video Technology, 1, 3, 247-256, (1991)
- [5] I. Pitas, A.N. Venetsanopoulos, Order statistics in digital image processing, Proceedings of IEEE, 80, 12, 1893-1923, (1992)
- [6] J. Astola, P. Haavisto, Y. Neuvo, Vector median filters, IEEE Proceedings, 78, 678-689, (1990)
- [7] 12. B. Smolka, K. Wojciechowski, Random walk approach to image enhancement, Signal Processing, Vol. 81, No. 4
- [8] G. Borgefors, Distances transformations in digital images. Computer Vision, Graphics and Image Processing, 34:334-371,1986
- [9] G. Matheron, Random Sets and Integral Geometry. John Wiley, New York, 1975
- [10] Henk J.A.M. Heijmans., Mathematical Morphology: Basic Principles, Proceedings of the Summer School on Morphological Image and Signal Processing, Zakopane, Poland, 1995

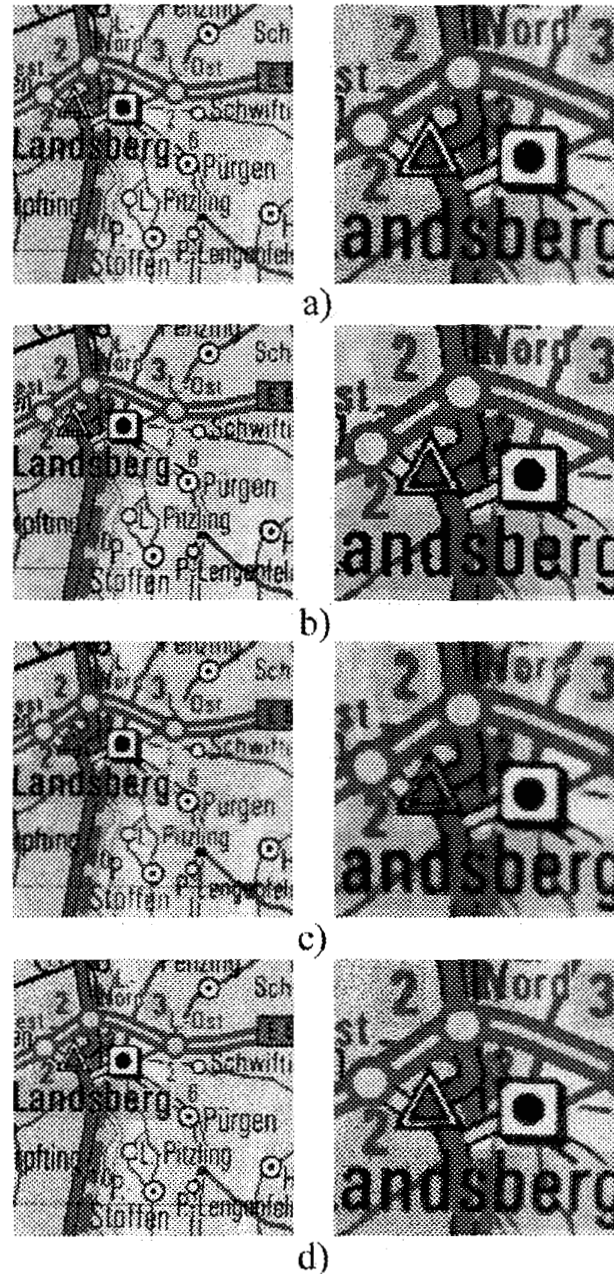


Fig. 2. Comparison of the efficiency of the vector median and the proposed filter: **a)** test image (part of a scanned map), **b)** result of the new filtering technique ($\beta = 20$, $\alpha = 1.25$, 3 iterations), **c)** result of the standard vector median filtration (3×3 mask), **d)** result of the DDF (3×3 mask).

METHOD _N	NMSE [10 ⁻³]	RMSE	SNR [dB]	PSNR [dB]	NCD [10 ⁻⁴]
NONE	502.410	28.683	12.989	18.978	244.190
AMF ₁	90.184	12.152	20.449	26.438	115.210
AMF ₃	88.815	12.060	20.515	26.504	99.043
AMF ₅	113.840	13.653	19.437	25.426	98.853
VMF ₁	168.830	16.627	17.725	23.714	158.920
VMF ₃	113.420	13.628	19.453	25.442	129.700
VMF ₅	105.180	13.124	19.781	25.770	123.390
BVDF ₁	372.320	24.691	14.291	20.280	153.420
BVDF ₃	363.390	24.394	14.396	20.385	129.040
BVDF ₅	367.740	24.539	14.345	20.334	124.350
GVDF ₁	144.640	15.390	18.397	24.386	127.370
GVDF ₃	99.400	12.758	20.026	26.015	97.348
GVDF ₅	100.490	12.828	19.979	25.968	92.583
DDF ₁	184.620	17.387	17.337	23.326	149.540
DDF ₃	127.260	14.436	18.953	24.942	120.400
DDF ₅	118.820	13.949	19.251	25.240	114.400
HDF ₁	147.060	15.518	18.325	24.314	139.380
HDF ₃	87.730	11.986	20.569	26.558	107.600
HDF ₅	79.698	11.424	20.986	26.975	101.140
AHDF ₁	131.390	14.668	18.814	24.803	137.650
AHDF ₃	78.739	11.355	21.038	27.027	106.180
AHDF ₅	72.331	10.883	21.407	27.396	99.673
FVDF ₁	103.950	13.047	19.832	25.821	112.450
FVDF ₃	72.888	10.925	21.373	27.362	89.743
FVDF ₅	77.012	11.230	21.134	27.123	88.023
ANMF ₁	112.660	13.583	19.482	25.471	120.270
ANMF ₃	80.934	11.512	20.919	26.908	96.789
ANMF ₅	84.101	11.735	20.752	26.741	93.171
ANP-E ₁	88.827	12.060	20.515	26.504	115.100
ANP-E ₃	79.688	11.423	20.986	26.975	100.860
ANP-E ₅	94.793	12.459	20.232	26.221	101.070
ANP-G ₁	88.787	12.058	20.517	26.506	115.080
ANP-G ₃	79.674	11.422	20.987	26.976	100.850
ANP-G ₅	94.741	12.455	20.235	26.224	101.050
ANP-D ₁	105.280	13.130	19.776	25.765	113.610
ANP-D ₃	73.211	10.949	21.354	27.343	89.078
ANP-D ₅	78.419	11.332	21.056	27.045	87.650
VBAMMF ₁	90.184	12.152	20.449	26.438	115.210
VBAMMF ₃	88.815	12.060	20.515	26.504	99.043
VBAMMF ₅	113.840	13.653	19.437	25.426	98.853
NEW ₁	65.412	10.349	21.843	27.832	95.248
NEW ₂	57.921	9.739	22.372	28.361	88.917
NEW ₃	61.473	10.033	22.113	28.102	88.561

Table 2. Comparison of the new algorithm with the standard techniques (Tab. 1) using the *PEPPERS* standard image corrupted by Gaussian noise $\sigma = 30$. The subscripts denote the iteration number.

METHOD _N	NMSE [10 ⁻³]	RMSE	SNR [dB]	PSNR [dB]	NCD [10 ⁻⁴]
NONE	905.930	42.674	10.429	15.528	305.550
AMF ₁	128.940	16.099	18.896	23.995	122.880
AMF ₃	97.444	13.996	20.112	25.211	95.800
AMF ₅	113.760	15.122	19.440	24.539	92.312
VMF ₁	161.420	18.013	17.920	23.019	161.700
VMF ₃	104.280	14.478	19.818	24.916	128.620
VMF ₅	96.464	13.925	20.156	25.255	121.790
BVDF ₁	354.450	26.692	14.504	19.603	152.490
BVDF ₃	336.460	26.006	14.731	19.829	123.930
BVDF ₅	338.940	26.102	14.699	19.797	118.500
GVDF ₁	140.970	16.833	18.509	23.607	126.820
GVDF ₃	93.444	13.705	20.294	25.393	94.627
GVDF ₅	91.118	13.534	20.404	25.503	89.277
DDF ₁	176.670	18.845	17.528	22.627	152.050
DDF ₃	119.330	15.488	19.232	24.331	119.940
DDF ₅	110.620	14.912	19.561	24.660	113.390
HDF ₁	143.190	16.966	18.441	23.539	139.360
HDF ₃	82.413	12.871	20.840	25.939	104.620
HDF ₅	74.487	12.236	21.279	26.378	97.596
AHDF ₁	132.710	16.333	18.771	23.869	138.180
AHDF ₃	75.236	12.298	21.236	26.334	103.410
AHDF ₅	68.563	11.740	21.639	26.738	96.327
FVDF ₁	108.760	14.786	19.635	24.734	111.220
FVDF ₃	73.796	12.179	21.320	26.418	83.629
FVDF ₅	76.274	12.382	21.176	26.275	80.081
ANMF ₁	110.720	14.919	19.558	24.656	113.560
ANMF ₃	75.652	12.332	21.212	26.310	86.836
ANMF ₅	76.757	12.421	21.149	26.247	82.825
ANP-E ₁	128.590	16.077	18.908	24.007	122.890
ANP-E ₃	90.509	13.488	20.433	25.532	97.621
ANP-E ₅	96.930	13.959	20.135	25.234	94.131
ANP-G ₁	128.600	16.078	18.908	24.006	122.900
ANP-G ₃	90.523	13.489	20.432	25.531	97.603
ANP-G ₅	96.990	13.963	20.133	25.231	94.134
ANP-D ₁	113.900	15.131	19.435	24.533	115.230
ANP-D ₃	74.203	12.213	21.296	26.394	85.026
ANP-D ₅	76.265	12.381	21.177	26.275	81.202
VBAMMF ₁	128.940	16.099	18.896	23.995	122.880
VBAMMF ₃	97.444	13.996	20.112	25.211	95.800
VBAMMF ₅	113.760	15.122	19.440	24.539	92.312
NEW ₁	74.762	12.259	21.263	26.362	83.585
NEW ₂	55.239	10.537	22.578	27.676	72.115
NEW ₃	56.078	10.617	22.512	27.611	70.008

Table 3. Comparison of the new algorithm with the standard techniques (Tab. 1) using the *LENA* standard image corrupted by 4% Impulse and Gaussian noise $\sigma = 30$. The subscripts denote the iteration number.